Experimental and Molecular Pathology 108 (2019) 80–88

Contents lists available at ScienceDirect

Experimental and Molecular Pathology

journal homepage: www.elsevier.com/locate/yexmp

Triptolide inhibits viability and migration while promotes apoptosis in nephroblastoma cells by regulation of miR-193b-3p

Shiying Hang[a,b,1], Xianghong Wang[a,1], Hai Li[a,*]

[a] Department of Pediatric Surgery, Jining No.1 People's Hospital, Jining 272011, China
[b] Affiliated Jining No.1 People's Hospital of Jining Medical University, Jining Medical University, Jining 272011, China

ARTICLE INFO

Keywords:
Nephroblastoma
Triptolide
miR-193b-3p
KLF4
PI3K/AKT/ERK

ABSTRACT

Background: Triptolide (TPL) is a potential anti-tumor natural compound. However, its role in nephroblastoma is poorly studied. Herein, we aimed to reveal the regulatory effects of TPL on human nephroblastoma cells (G-401 and WiT49) as well as the regulatory mechanism in G-401 cells.

Methods: Effects of TPL on cell viability, migration and apoptosis of G-401 and WiT49 cells were measured by CCK-8 assay, Boyden Chamber, and flow cytometry/Western blot analysis, respectively. Expression of miR-193b-3p in TPL-treated G-401 and WiT49 cells was determined by RT-qPCR. Then, whether miR-193b-3p was the downstream factor of TPL was studied. Alteration of KLF4 expression in TPL-treated cells and the relationship between miR-193b-3p and KLF4 were assessed by Western blot analysis and luciferase reporter assay. Effects of abnormally expressed KLF4 on G-401 cells were also assessed. Finally, the involvements of PI3K/AKT and ERK pathways were measured by Western blot analysis.

Results: TPL reduced cell viability and migration while promoted apoptosis in G-401 and WiT49 cells. miR-193b-3p level was up-regulated by TPL stimulation, and TPL might function through regulation of miR-193b-3p. KLF4 expression was down-regulated by TPL, and KLF4 was proven to be a target gene of miR-193b-3p. TPL mediated the repressive roles in growth of nephroblastoma cells via KLF4 knockdown. Finally, we found phosphorylation of PI3K, AKT and ERK was inhibited by TPL, possibly through miR-193b-3p-mediated regulation of KLF4.

Conclusion: TPL showed a tumor suppressive role in nephroblastoma cells via miR-193b-3p-mediated down-regulation of KLF4, along with inhibition of the PI3K/AKT and ERK pathways.

1. Introduction

Nephroblastoma, also termed Wilms tumor, ranks the second among the abdominal solid tumors in children (Richards et al., 2017). Annually, the incidence rate of nephroblastoma reaches 1/10000 among children younger than 15 years worldwide, and 98% of those cases occurred in children before the age of 10 years (Breslow et al., 1993; Emerson et al., 2004). There are two treatment approaches available for patients with nephroblastoma, including chemotherapy-resection-adjuvant therapy conducted by the Children's Oncology Group (COG) in North America and immediate surgery conducted by the International Society of Pediatric Oncology (SIOP) in Europe (D'Angio, 2008). After treatments, the five-year survival rate has been improved to over 90% currently (Hu et al., 2016b). However, tumor progression or recurrence after treatments can be observed in 10–15% of patients, and 25% of the survivors may live with serious chronic health conditions 25 years later (Sarin and Raj, 2015; Tian et al., 2014). Therefore, innovative drugs for treatment of nephroblastoma as well as the underlying mechanisms are of utmost importance and highly warranted.

Triptolide (TPL), a highly oxygenated diterpene, is a key ingredient from the Chinese herb *Tripterygium wilfordii* (Zhang et al., 2018). It has been used in traditional Chinese medicine to treat autoimmune and inflammatory diseases for centuries (Ziaei and Halaby, 2016). Recently, more and more evidence has pointed out that TPL possesses an anti-cancer property both in vitro and in vivo. For example, orthotopic growth of lung cancer cells in rats was reduced by TPL, and proliferation, cell viability and self-renewal of lung cancer cells were suppressed by TPL (Song et al., 2017). A previous study has shown that TPL can decrease cell viability and promote apoptosis in liver cancer cells by activating p53, a tumor suppressor gene (Sun et al., 2017). In addition, TPL was proven to repress viability, migration and invasion of pituitary adenoma cells with the involvements of the ADAM12/EGFR signaling

* Corresponding author at: Department of Pediatric Surgery, Jining No.1 People's Hospital, No.6 Jiankang Road, Jining 272011, China.
E-mail address: haili0013@sina.com (H. Li).
[1] Co-first authors.

https://doi.org/10.1016/j.yexmp.2019.04.006
Received 14 September 2018; Received in revised form 25 February 2019; Accepted 8 April 2019
Available online 09 April 2019
0014-4800/

cascade (Wang et al., 2018). However, the potential role of TPL in nephroblastoma cells remains unclear, which needs more attention.

microRNAs (miRNAs/miRs) are non-coding RNAs with a length of about 22 nucleotides. These single stranded RNAs are identified to be deregulated in cancer cells and act as a tumor suppressor or an oncogene, affecting cancer malignancy (Li et al., 2016a). miR-193b-3p has been proved as a tumor suppressor by targeting oncogenes in several malignant tumors (Li et al., 2014; Okuda et al., 2013). In addition, several studies described previously have attributed the anti-tumor effects of TPL to the downstream miRNAs, such as miR-21 (Li et al., 2016b) and miR-181a (Jiang et al., 2018). Hence, the downstream miRNAs might be a rational direction for the study of molecular mechanism underlying TPL. Kruppel-like factor (KLF4) has been reported to be highly expressed in multiple cancer cells and exhibits accelerative effects on the development of malignancies (Le Magnen et al., 2013; Tetreault et al., 2010; Yu et al., 2011). Particularly, its modulatory function is mediated by several miRs in the pathological progress of cancers (Davis-Dusenbery et al., 2011; Okuda et al., 2013). However, it is still incompletely understood whether the regulatory correlation between miR-193-3p and KLF4 occurred in the nephroblastoma cells under TPL-treated context.

Here, we analyzed the alteration of cell viability, migration and apoptosis after TPL treatment in human nephroblastoma G-401 and WiT49 cells. Additionally, miR-193b-3p was quantified in TPL-treated G401 and WiT49 cells. To figure out the regulatory mechanism, the correlation between TPL treatment and the target gene of miR-193b-3p was studied in TPL-treated G-401 cells. In addition, the involvements of the possibly associated signaling pathway were also investigated.

2. Materials and methods

2.1. Cell culture and treatment

The human malignant rhabdoid kidney tumor cell line, G-401 (ATCC® CRL-1441™), was obtained from American Type Culture Collection (ATCC; Manassas, VA, USA). G-401 cells were maintained in ATCC-formulated McCoy's 5a Medium Modified (ATCC) supplemented with 10% fetal bovine serum (FBS; Hyclone, Little Chalfont, UK). For cell growth, G-401 cells were subjected to a humidified incubator at 37 °C with 5% CO_2, and the culture medium was renewed 2 to 3 times per week. WiT49 cells were obtained from Jining No.1 People's Hospital, which were cultured according to previously reported method (Li et al., 2008). Briefly, WiT49 cells were cultured in Dulbecco's modified Eagle medium (DMEM)/Ham's nutrient mixture F12 (1:1) (Sigma-Aldrich, St. Louis, MO, USA), 10% FBS, 100 U/mL penicillin (Sigma), and 100 μg/mL streptomycin (Sigma).

TPL, the purity of which was ≥98% (HPLC), was purchased from (Sigma-Aldrich). TPL was dissolved in dimethyl sulfoxide (DMSO) to generate a stock solution with a concentration of 10 mM, and the stock solution was stored at −20 °C. TPL was diluted from the stock solution into FBS-free medium to 5, 10, 25 and 50 nM and applied to stimulate cells for 72 h. The percentage of DMSO in the diluent was below 1%.

2.2. Cell transfection with miRNAs

miR-193b-3p inhibitor and its negative control (NC) were obtained from GenePharma Co. (Shanghai, China). miR-193b-3p inhibitor was transfected into G-401 cells for inhibition of miR-193b-3p using Lipofectamine 3000 reagent (Thermo Fisher Scientific, Inc., Waltham, MA, USA). Cell transfection was performed according to the manufacturer's protocol, and cells transfected with NC were acted as control.

2.3. Cell transfection with plasmids

Full-length KLF4 sequences and short-hairpin RNA directed against KLF4 were cloned into the pEX-2 and pGPU6/Neo plasmids (GenePharma), respectively. After sequencing, these reconstructed plasmids were referred to as pEX-KLF4 and sh-KLF4, respectively. The pGPU6/Neo plasmid carrying a non-targeting sequence was used as a negative control of sh-KLF4, which was termed sh-NC. Empty pEX-2 plasmid was used as a negative control of pEX-KLF4. The plasmids talked above were transfected into G-401 cells using the lipofectamine 3000 reagent, followed by selection in culture medium containing 0.5 mg/mL G418 (Sigma-Aldrich). Stably transfected cells were obtained after approximately 4 weeks and then stimulated with TPL.

2.4. Measurement of cell viability in vitro

Cell viability was assessed by the cell counting kit-8 (CCK-8) assay. In brief, approximately 5×10^3 cells were seeded into each well of 96-well plates. Then, cells were incubated at 37 °C overnight for attachment. After treatments, 10 μL of CCK-8 reagent, provided by Dojindo Molecular Technologies (Kumamoto, Japan), was added into each well, and the 96-well plates were subjected into a humidified incubator for another 1 h at 37 °C. The OD values at 450 nm were detected by using a Microplate Reader (Bio-Rad, Hercules, CA, USA).

2.5. Measurement of apoptosis in vitro

Identification and detection of apoptotic cells were executed using the Annexin V-FITC Apoptosis Detection Kit (Solarbio), as suggested by the manufacturer. Cells (1×10^6 cells/mL) were plated into 6-well plates and incubated at 37 °C overnight for attachment. After treatments, cells were harvested, washed with PBS, and resuspended in binding buffer. Then, cells were stained with 5 μL Annexin V-FITC and 5 μL propidium iodide at room temperature in the dark. Apoptotic cells were detected using a flow cytometer (BD FACSVerse; BD Biosciences, San Jose, CA, USA), and percentage of apoptotic cells was assessed by the Cell Quest software (Becton-Dickinson, San Jose, CA, USA).

2.6. Measurement of migration in vitro

Cell migration was evaluated by Boyden Chamber assay according to previous method (Sun et al., 2016). In brief, after treatments, cells suspended in 200 μL of FBS-free medium were seeded in the upper chamber in 24-well plate with an 8 μm pore (Millipore, Temecula, CA, USA). The lower chamber was filled with 800 μL of FBS-free complete medium. After incubation at 37 °C for 12 h, cells were removed from the upper chamber and fixed with 4% formalin for 25 min. Then, cells in five fields were counted under a microscope (Olympus, Center Valley, PA, USA).

2.7. Luciferase reporter assay

The correlation between miR-193b-3p and KLF4 was studied in HEK293 cells (ATCC). The 3′-untranslated region (3'UTR) of KLF4, which carries a miR-193b-3p-binding site, was ligated into the downstream of luciferase gene in pMIR-REPORT vector (Ambion, Austin, TX, USA) to generate Luc-KLF4-wt (KLF4-wt). In the meantime, the putative miR-193b-3p-binding site in KLF4-wt was mutated by site-directed mutagenesis, and the mutated plasmid was referred to as KLF4-mt. HEK293 cells were co-transfected with miR-193b-3p mimic (scramble miRNA, both synthesized by GenePharma) and KLF4-wt (KLF4-mt) using Lipofectamine 3000 reagent. Luciferase activity was assessed at 48 h post-transfection using the dual-luciferase assay system (Promega), as suggested by the manufacturer.

2.8. Reverse transcription-quantitative PCR (RT-qPCR)

After treatments, total RNAs of cells were extracted using a Qiagen RNA isolation kit (RNeasy, Qiagen, Valencia, CA, USA) following the manufacturer's instructions. The RNA pellet was suspended in RNase-

free distilled water, followed by measurements of the purity and concentration. Then, with the help of the Taqman MicroRNA Reverse Transcription Kit (Applied Biosystems, Foster City, CA, USA), 50 ng RNA was reversely transcribed into cDNA according to the manufacturer's protocol. The Taqman Universal Master Mix II (Applied Biosystems) was utilized for real-time PCR to quantify miR-193b-3p. Amplification was performed on an ABI 7500 Real-Time PCR system (Applied Biosystems) with the following cycling conditions: 95 °C for 10 min, followed by 40 cycles of 95 °C for 15 s and 60 °C for 1 min. The relative expression of miR-193b-3p was calculated using the comparative cycle threshold (Ct) method ($2^{-\Delta\Delta Ct}$) (Livak and Schmittgen, 2001) with U6 as the endogenous control to normalize the data.

2.9. Western blot analysis

After treatments, cells were harvested and lysed in RIPA buffer (Beyotime, Shanghai, China). The protein extracts were centrifuged at 12000*g* for 15 min, and the supernatant was loaded onto SDS-PAGE gels after quantification of protein concentration using the BCA™ Protein Assay Kit (Pierce, Appleton, WI, USA). After separation by SDS-PAGE, proteins were transferred to nitrocellulose membranes. The membranes were blocked with 5% bovine serum albumin (BSA) in Tris-buffered saline, and were incubated with primary antibodies and HRP-conjugated secondary antibody (goat anti-rabbit, ab205718, Abcam, Cambridge, UK), successively. Primary antibodies included antibodies against cleaved caspase-3 (ab2302), cleaved caspase-9 (ab2324), Bcl-2 (ab32124), Bax (ab32503), Krüppel-like factor 4 (KLF4; ab106629), total (t)-PI3K (ab191606), phospho (p)-PI3K (ab182651), t-ERK (ab17942), p-ERK (ab214362), β-actin (ab8227, all Abcam), t-AKT (#9272) or p-AKT (#9271, both Cell Signaling Technology, Beverly, MA, USA). Finally, the protein bands were visualized using the enhanced chemiluminescence kit (Amersham Biosciences, Piscataway, New Jersey, USA). The intensity of the bands was determined by ImageJ software (National Institutes of Health, Bethesda, MA, USA).

2.10. Statistical analysis

Experiments were performed in triplicate with three repeats. The results were presented as the mean ± standard deviation (SD). All data were analyzed using Graphpad Prism 6 software (GraphPad, San Diego, CA, USA). The statistical difference was assessed using the unpaired two-tailed *t*-test or one-way analysis of variance (ANOVA). *P* value < .05 was considered statistically significant.

3. Results

3.1. TPL inhibited cell viability and migration while promoted apoptosis in G-401 and WiT49 cells

Effects of TPL on cell viability, migration and apoptosis were studied. According to the results of CCK-8 assay, cell viability of G-401 and WiT49 cells was significantly reduced by 10 nM TPL ($P < .05$), 25 nM TPL ($P < .01$) and 50 nM TPL ($P < .001$, Fig. 1A and B). Cell viability was reduced to a half when they were stimulated with 25 nM TPL; hence, cells were stimulated with 25 nM TPL in subsequent experiments. Similarly, cell migration was also markedly decreased by TPL stimulation ($P < .01$, Fig. 1C and D). In Fig. 1E and G, percentage of apoptotic cells in the TPL group was remarkably higher than that in the Control group ($P < .001$). Western blot analysis in Fig. 1F and H showed TPL observably induced expression of cleaved caspase-3 and cleaved caspase-9, up-regulated Bax expression, and down-regulated Bcl-2 expression. Results collectively illustrated that TPL could repress cell viability and migration while promote apoptosis in G-401 and WiT49 cells.

3.2. TPL up-regulated miR-193b-3p expression

Expression of miR-193b-3p after TPL stimulation was evaluated. Fig. 2A and B showed levels of miR-193b-3p were notably elevated by 10 nM TPL ($P < .05$) and 25–50 nM TPL (both $P < .01$). Results illustrated that TPL could up-regulate miR-193b-3p expression in G-401 and WiT49 cells.

3.3. TPL affected G-401 cells through up-regulating miR-193b-3p expression

Whether miR-193b-3p was a downstream factor of TPL was studied subsequently. Results in Fig. 3A showed miR-193b-3p expression was prominently down-regulated in cells transfected with miR-193b-3p inhibitor compared with the NC-transfected cells ($P < .01$), suggesting that miR-193b-3p could be silenced successfully after cell transfection. Notably, miR-193b-3p silence per se augmented cell viability ($P < .05$, Fig. 3B) and migration behaviors ($P < .05$, Fig. 3C) as well as impeded apoptosis at least in part (Fig. 3D-E) in comparision with its negative control. Then, effects of miR-193b-3p inhibition on alterations induced by TPL were further investigated. Results implied effects of TPL were attenuated by miR-193b-3p inhibition relative to negative control, as cell viability was significantly increased ($P < .05$, Fig. 3B), migration was markedly enhanced ($P < .05$, Fig. 3C), apoptotic cells were notably lowered ($P < .05$, Fig. 3D), expression of cleaved caspase-3, cleaved caspase-9 and Bax was down-regulated, and expression of Bcl-2 was up-regulated (Fig. 3E), when compared to the TPL + NC group. Results collectively proposed that TPL might affect G-401 cells via up-regulation of miR-193b-3p.

3.4. KLF4 was a target of miR-193b-3p

Next, the possible target gene of miR-193b-3p was explored. Western blot analysis in Fig. 4A–B showed KLF4 protein expression was markedly down-regulated by 25–50 nM TPL (both $P < .01$), presenting an inverse trend after TPL stimulation compared with miR-193b-3p. Results in Fig. 4C–D showed KLF4 protein level in cells transfected with miR-193b-3p inhibitor was prominently higher than that in NC-transfected cells ($P < .01$), suggesting a negative correlation between miR-193b-3p and KLF4 expression. In Fig. 4E, luciferase activity was significantly reduced by miR-193b-3p mimic in cells transfected with KLF4-wt ($P < .05$), while the effects of miR-193b-3p mimic on luciferase activity were non-significant in cells transfected with KLF4-mt. Results collectively supported that KLF4 was a target of miR-193b-3p.

3.5. Effects of KLF4 knockdown on G-401 cells were consistent with that of TPL

Effects of abnormally expressed KLF4 on cell viability, migration and apoptosis were studied to illustrate whether the alteration of KLF4 was an explanation for the effects of TPL on G-401 cells. In Fig. 5A, KLF4 protein levels in cells transfected with pEX-KLF4 were notably higher than that in pEX-2-transfected cells ($P < .01$). Meanwhile, KLF4 protein levels in cells transfected with sh-KLF4 were significantly lower than that in sh-NC-transfected cells ($P < .01$). Results illustrated that stable transfection with recombined plasmid could alter expression level of KLF4 successfully. Afterwards, we found KLF4 overexpression could effectively increase cell viability ($P < .05$, Fig. 5B) and migration ($P < .01$, Fig. 5C), whereas KLF4 knockdown showed the opposite effects on viability and migration (both $P < .05$). Furthermore, we verified that the repressive functions of TPL on cell viability and migration were distinctly suppressed in G-401 cells transfected with pEX-KLF4 ($P < .05$ or $P < .01$, Fig. 5B and C). Results showed non-significant effects of KLF4 overexpression on apoptotic cells (Fig. 5D) and expression of apoptosis-associated proteins (Fig. 5E). However, KLF4 knockdown could dramatically elevate percentage of apoptotic cells

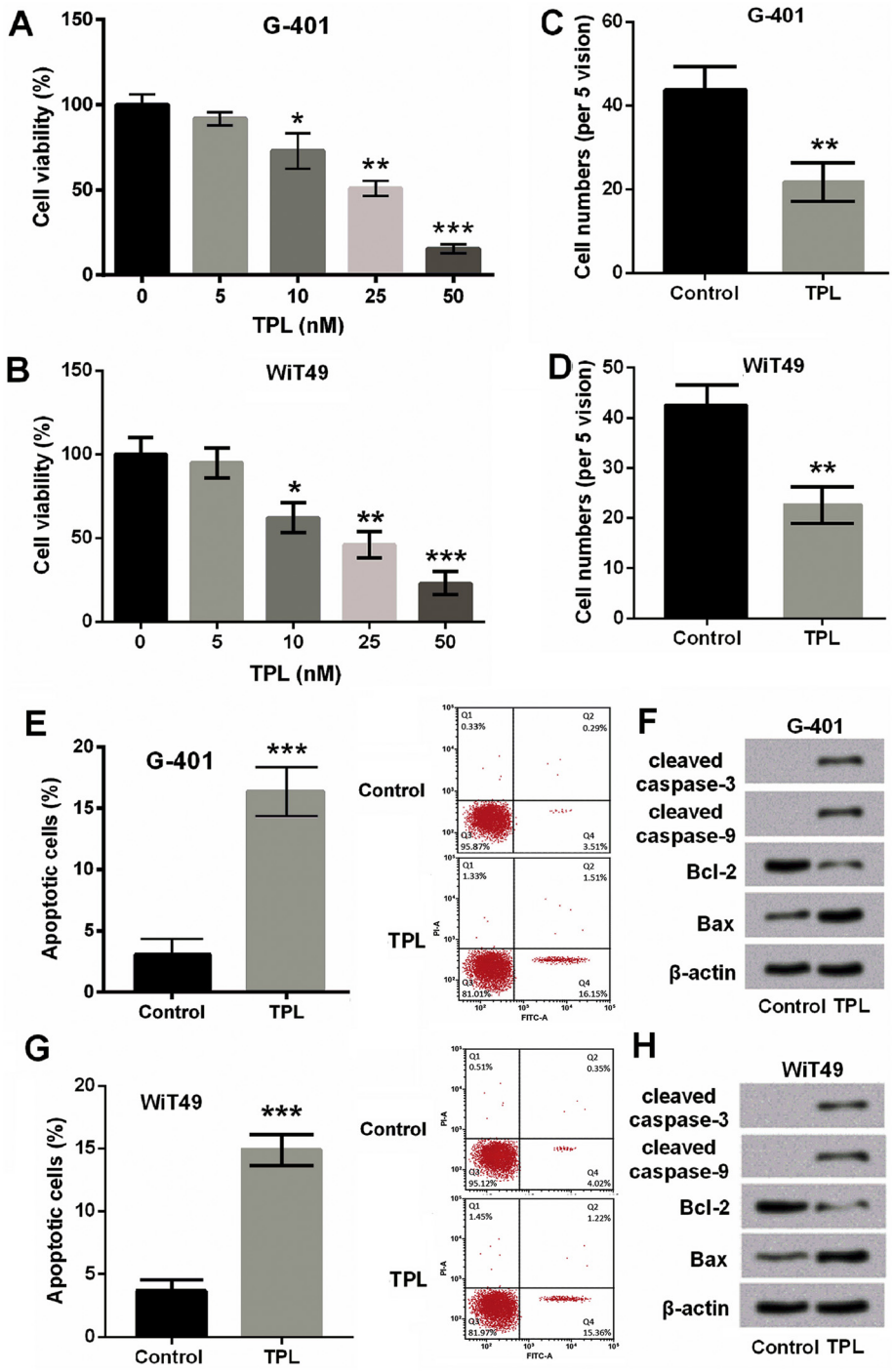

Fig. 1. Triptolide (TPL) reduced cell viability and migration while promoted apoptosis in G-401 and WiT49 cells. G-401 and WiT49 cells were stimulated with 0, 5, 10, 25 or 50 nM TPL, and cells treated with 0 nM TPL were acted as control. (A, B) Cell viability of G-401 and WiT49 cells was determined by CCK-8 assay, showing that TPL reduced cell viability. G-401 and WiT49 cells were stimulated with 25 nM TPL, and untreated cells were acted as control. (C, D) Relative cell migration of G-401 and WiT49 was evaluated by Boyden Chamber, showing that TPL repressed cell migration. (E, G) Percentage of apoptotic G-401 and WiT49 cells was analyzed by flow cytometry assay, showing that TPL promoted apoptosis. (F, H) Expression of apoptosis-associated proteins was measured by Western blot, showing that TPL promoted apoptosis of G-401 and WiT49 cells. Data are presented as the mean ± SD of three independent experiments. *, $P < .05$; **, $P < .01$; ***, $P < .001$.

($P < .001$), and effects of KLF4 knockdown on expression of apoptosis-associated proteins were consistent with that on apoptotic cells. In addition, the pro-apoptotic function of TPL was abolished in G-401 cells which were transfected with pEX-KLF4 ($P < .05$ or $P < .001$, Fig. 5D and E). Results talked above demonstrated that TPL exhibited an inhibitory effect on the growth of nephroblastoma cells via down-regulating KLF4.

3.6. TPL inhibited the PI3K/AKT and ERK pathways via miR-193b-3p-mediated regulation of KLF4

Effects of TPL on signaling cascades were finally studied. Results in Fig. 6A showed phosphorylation levels of PI3K, AKT and ERK were all prominently reduced by TPL stimulation relative to the control group (all $P < .05$). Those reductions could be markedly reversed by miR-193b-3p inhibition (all $P < .05$), suggesting that TPL might inhibit the PI3K/AKT and ERK pathways via regulation of miR-193b-3p. Results in Fig. 6B showed phosphorylation levels of PI3K, AKT and ERK were significantly enhanced by KLF4 overexpression ($P < .05$ or $P < .01$) while were markedly reduced by KLF4 knockdown (all $P < .05$). Collectively, we concluded that TPL might inhibit the PI3K/AKT and ERK pathways through miR-193b-3p-mediated regulation of KLF4 in G-401 cells.

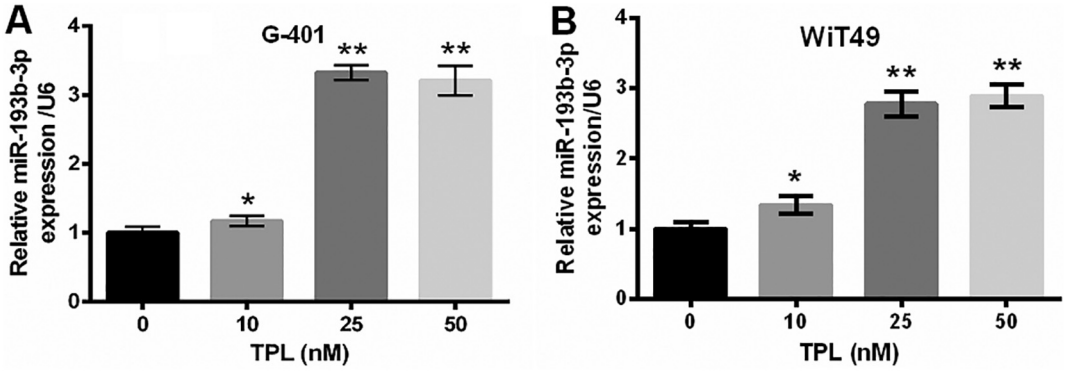

Fig. 2. Triptolide (TPL) up-regulated miR-193b-3p expression in G-401 and WiT49 cells. (A) G-401 cells and (B) WiT49 cells were stimulated with 0, 10, 25 or 50 nM TPL, and cells treated with 0 nM TPL were acted as control. Expression of miR-193b-3p was determined by RT-qPCR, showing that TPL elevated miR-193b-3p levels. Data are presented as the mean ± SD of three independent experiments. *, $P < .05$; **, $P < .01$.

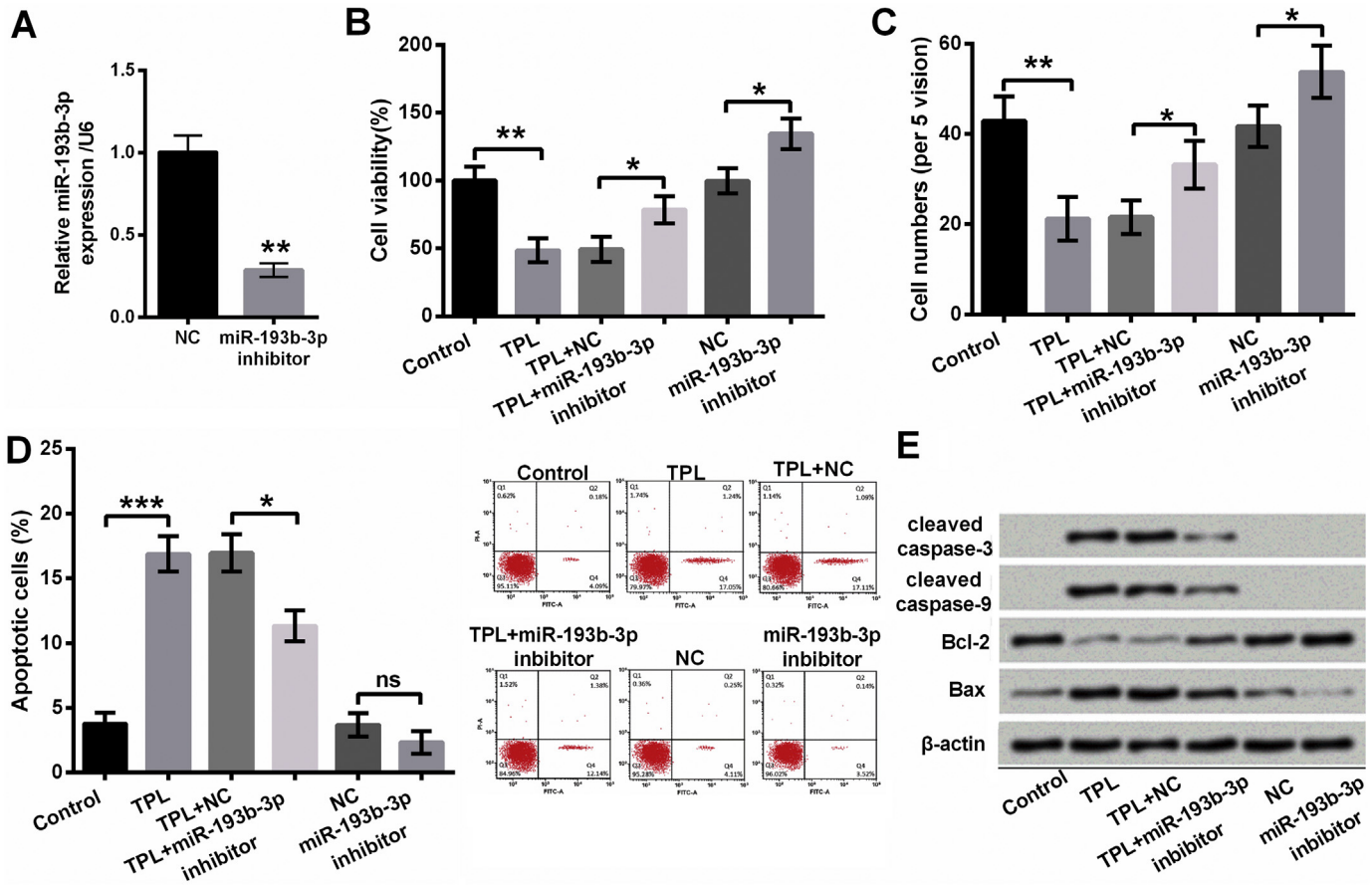

Fig. 3. Triptolide (TPL) affected G-401 cells through up-regulating miR-193b-3p. G-401 cells were transfected with miR-193b-3p inhibitor or its negative control (NC). (A) Expression of miR-193b-3p was determined by RT-qPCR, showing that miR-193b-3p was successfully silenced after cell transfection. G-401 cells (transfected or untransfected) were stimulated with 25 nM TPL, and untreated cells were acted as control. (B) Cell viability was assessed by CCK-8 assay, showing that miR-193b-3p inhibition abolished the inhibitory effects of TPL on cell viability. (C) Relative cell migration was evaluated by Boyden Chamber, showing that miR-193b-3p inhibition promoted cell migration which was retarded by TPL. (D) Percentage of apoptotic cells was analyzed by flow cytometry assay, showing miR-193b-3p inhibition repressed apoptosis which was promoted by TPL. (E) Expression of apoptosis-associated proteins was measured by Western blot, showing miR-193b-3p inhibition repressed apoptosis which was induced by TPL. Data are presented as the mean ± SD of three independent experiments. *, $P < .05$; **, $P < .01$; ***, $P < .001$.

4. Discussion

Nephroblastoma is the most common malignancy in the kidney of children, along with high cure rates. However, the relapse after treatments may lead to dismal outcome (Sarin and Raj, 2015). Herein, we found TPL might be a potential drug for treatment of nephroblastoma as it could repress cell viability and migration while promote apoptosis of G-401 and WiT49 cells. We further proposed that TPL affected G-401 and WiT49 cells through up-regulating miR-193b-3p expression. In addition, the miR-193b-3p-induced down-regulation of KLF4 was proven to be an explanation for the effects of TPL on G-401 cells. Finally, we found TPL could inhibit the PI3K/AKT and ERK pathways through miR-193b-3p-mediated regulation of KLF4.

Uncontrolled growth and spread of cells are chief concerns of cancer

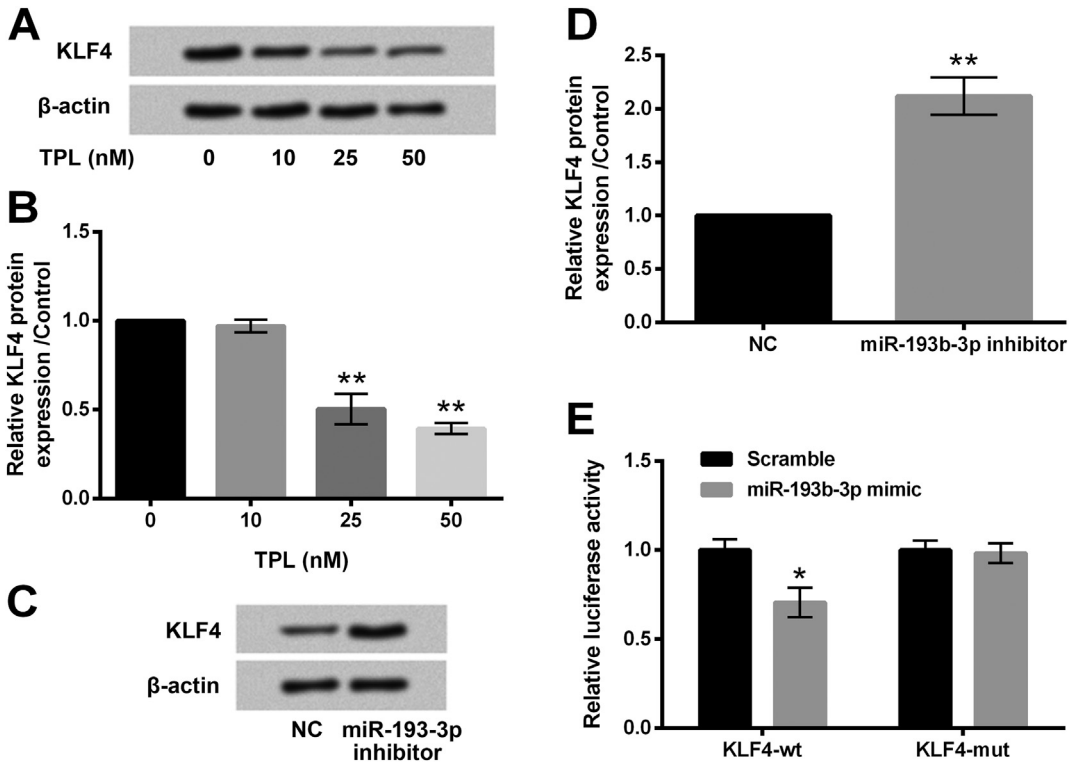

Fig. 4. KLF4 was a target gene of triptolide (TPL). G-401 cells were stimulated with 0, 10, 25 or 50 nM TPL, and cells treated with 0 nM TPL were acted as control. (A-B) Protein expression of KLF4 was measured by Western blot analysis, showing that TPL down-regulated KLF4 expression. G-401 cells were transfected with miR-193b inhibitor or its negative control (NC). (C-D) Protein expression of KLF4 was measured by Western blot analysis, showing that miR-193b-3p inhibition up-regulated KLF4 expression (E) Relative luciferase activity was analyzed by luciferase reporter assay, showing a direct targeting between miR-193b-3p and KLF4 3'UTR. Data are presented as the mean ± SD of three independent experiments. *, $P < .05$; **, $P < .01$.

(Prabhu et al., 2015). There is overwhelming evidence that TPL shows pleiotropic anti-tumor activities in cancer cells through repressing cell growth and promoting migration. Hu et al. have reported that TPL significantly suppresses cell viability and induces apoptosis of human ovarian carcinoma-derived COC1/DDP cells (Hu et al., 2016a). Li et al. have proposed that TPL represses growth of human breast cancer MCF-7 cells both in vitro and in vivo (Li et al., 2015). Reno et al. have also implied that migration, invasion and metastasis of lung cancer cells are suppressed by TPL (Reno et al., 2015). In our study, we firstly studied the effects of TPL on G-401 and WiT49 cells focusing on the alteration of cell viability, migration and apoptosis. Results showed an inhibitory effect of TPL on viability and migration of G-401 and WiT49 cells and a promoting effect of TPL on apoptosis of G-401 and WiT49 cells, which was consistent with that reported in literatures described above. A previous study has proven that the caspase-3-dependent apoptosis is activated by TPL (Guan et al., 2017). Similarly, in our study, up-regulation of Bax, down-regulation of Bcl-2, and activation of caspase-9 and caspase-3 were observed in TPL-treated cells.

A growing body of research has focused on the contribution of miR-193b-3p in cancer cells. miR-193b-3p promoted cell proliferation in glioma cells (Zhong et al., 2014) and drove tumor progression in head and neck squamous cell carcinomas (Lenarduzzi et al., 2013). Conversely, miR-193b-3p possessed an anti-tumor activity in ovarian cancer cells (Zhang et al., 2017) and hepatocellular carcinoma cells (Xu et al., 2010). Since the regulatory mechanism of TPL in cancer cells is proven to be associated with miRNAs, therefore, we focused on the correlation between miR-193b-3p and TPL stimulation in subsequent experiments. Accordingly, the up-regulation of miR-193b-3p in TPL-treated cells suggested a possible involvement of miR-193b-3p on TPL-associated modulation both in G-401 and WiT49 cells. In addition, we also found TPL-induced alterations of cell viability, migration and apoptosis were effectively attenuated by miR-193b-3p inhibition. That is to say, up-regulation of miR-193b-3p after TPL stimulation might be a reason for the effects of TPL on G-401 cells.

KLF4 is related to both tumor suppression and oncogenesis. The repression of p53 expression by acting on the promoter of p53 is reported to be an oncogenic mechanism of KLF4 (Rowland et al., 2005). The tumor suppressive effects of TPL on other cancer cells are widely attributed to the association with p53 (Sun et al., 2017; Wang et al., 2014). Therefore, we hypothesized there might be a correlation between TPL and KLF4 expression. Results in our study proved the hypothesis and illustrated that TPL could down-regulate KLF4 expression. Commonly, miRNAs participate in multiple biological processes through base pairing to the 3'UTR of the target mRNA, resulting in degradation of mRNA and inhibition of translation (Guo et al., 2010). Several genes have been proven to be the target gene of miR-193b-3p in previous literatures, such as p21-activated kinase 3 (Zhang et al., 2017) and MYB oncogene (Mets et al., 2015). Hence, we speculated that there might be a relationship between miR-193b-3p and KLF4. Subsequent experiments in our study elucidated that KLF4 was a target gene of miR-193b-3p, and KLF4 knockdown acted a tumor suppressive role in G-401 cells, which was consistent with TPL stimulation.

Previous studies have reported that several molecular pathways are involved in the TPL-associated modulation in cancer cells. Activation of AKT, the downstream factor of PI3K, is inhibited by TPL in human breast cancer cells (Xiong et al., 2016). The phosphorylation levels of AKT and ERK are both decreased by TPL in human lung cancer cells (Song et al., 2017). Consistent with studies described above, these two pathways in our study were both inhibited by TPL stimulation. More experiments also illustrated that miR-193b-3p-mediated down-regulation of KLF4 might be an explanation for the inhibition of these two signaling pathways.

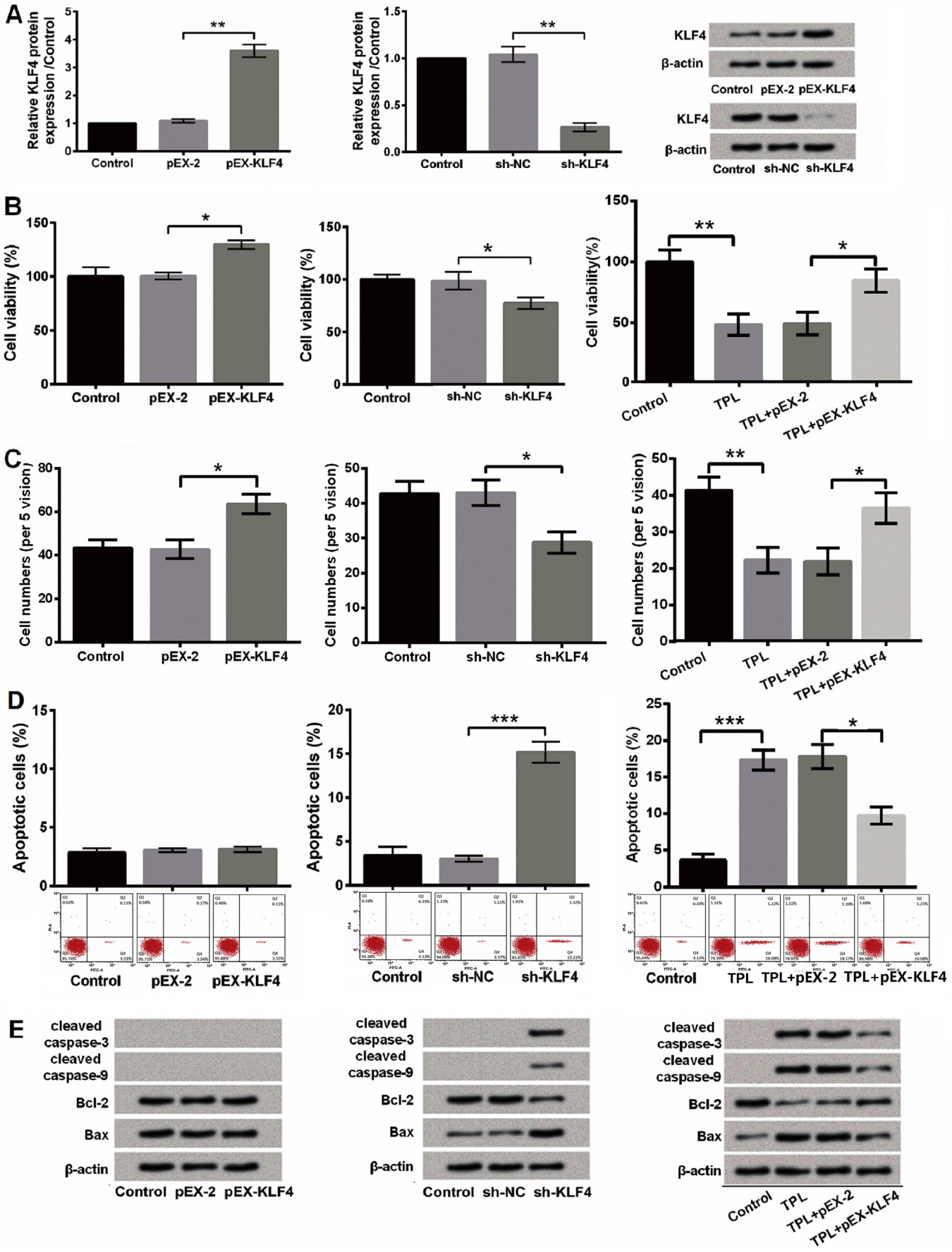

(caption on next page)

Fig. 5. KLF4 knockdown reduced cell viability and migration while promoted apoptosis in G-401 cells. G-401 cells were transfected with pEX-2, pEX-KLF4, sh-NC or sh-KLF4, and untreated cells were acted as control. (A) Protein expression of KLF4 was measured by Western blot analysis, showing that KLF4 expression was abnormally expressed after cell transfection. (B) Cell viability was assessed by CCK-8 assay, showing that TPL reduced cell viability via KLF4 knockdown. (C) Relative cell migration was evaluated by Boyden Chamber, showing that TPL repressed cell migration via KLF4 knockdown. (D) Percentage of apoptotic cells was analyzed by flow cytometry assay, showing that TPL promoted apoptosis via KLF4 knockdown. (E) Expression of apoptosis-associated proteins was measured by Western blot analysis, showing that TPL promoted apoptosis via KLF4 knockdown. Data are presented as the mean ± SD of three independent experiments. *, $P < .05$; **, $P < .01$; ***, $P < .001$.

5. Conclusions

We reported for the first time that TPL acted as a tumor suppressor in G-401 and WiT49 cells through inhibiting cell viability and migration while promoting apoptosis. TPL could up-regulate miR-193b-3p, and miR-193b-3p-induced down-regulation of KLF4 might be a reason for the tumor suppressive role of TPL. We also identified that TPL inhibited the PI3K/AKT and ERK pathways via miR-193b-3p-mediated regulation of KLF4. This study showed an innovative regulatory mechanism of TPL in cancer cells, assisting in application of TPL as a therapeutic drug of nephroblastoma. More evidence from animal experiments is needed to support the conclusion.

Acknowledgements

None.

Funding

This research did not receive any specific grant from funding agencies in the public, commercial, or not-profit sectors.

Conflict of interest statement

The authors declare that they have no conflicts of interest with the contents of this article.

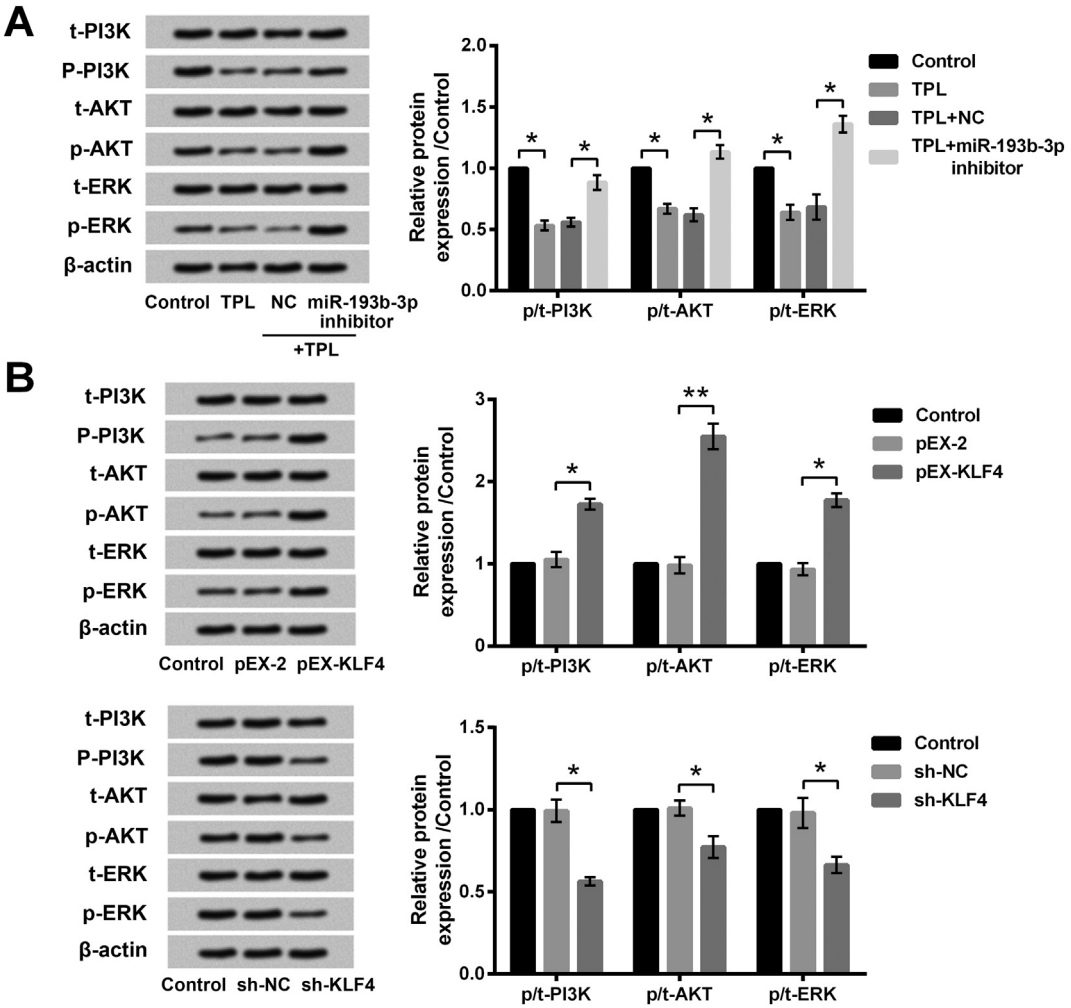

Fig. 6. Triptolide (TPL) inhibited the PI3K/AKT and ERK pathways via a miR-193b-3p-mediated regulation of KLF4 in G-401 cells. G-401 cells (transfected or untransfected) were stimulated with 25 nM TPL, and untreated cells were acted as control. (A) Protein expression of key kinases in the PI3K/AKT and ERK pathways was measured by Western blot analysis, showing that TPL inhibited the PI3K/AKT and ERK pathways via up-regulating miR-193b-3p. G-401 cells were transfected with pEX-2, pEX-KLF4, sh-NC or sh-KLF4, and untreated cells were acted as control. (B) Protein expression of key kinases in the PI3K/AKT and ERK pathways was measured by Western blot analysis, showing that the PI3K/AKT and ERK pathways were activated by KLF4 overexpression while were inhibited by KLF4 knockdown. Data are presented as the mean ± SD of three independent experiments. *, $P < .05$; **, $P < .01$.

References

Breslow, N., et al., 1993. Epidemiology of Wilms tumor. Med. Pediatr. Oncol. 21, 172–181.

D'Angio, G.J., 2008. Pre- or postoperative therapy for Wilms' tumor? J. Clin. Oncol. 26, 4055–4057.

Davis-Dusenbery, B.N., et al., 2011. Down-regulation of Kruppel-like factor-4 (KLF4) by microRNA-143/145 is critical for modulation of vascular smooth muscle cell phenotype by transforming growth factor-beta and bone morphogenetic protein 4. J. Biol. Chem. 286, 28097–28110.

Emerson, R.E., et al., 2004. Nephroblastoma arising in a germ cell tumor of testicular origin. Am. J. Surg. Pathol. 28, 687–692.

Guan, J., et al., 2017. Triptolide induces DNA breaks, activates caspase-3-dependent apoptosis and sensitizes B-cell lymphoma to poly(ADP-ribose) polymerase 1 and phosphoinositide 3-kinase inhibitors. Oncol. Lett. 14, 4965–4970.

Guo, H., et al., 2010. Mammalian microRNAs predominantly act to decrease target mRNA levels. Nature. 466, 835–840.

Hu, H., et al., 2016a. Anti-cancer and sensibilisation effect of triptolide on human epithelial ovarian cancer. J. Cancer 7, 2093–2099.

Hu, J., et al., 2016b. MicroRNA-197 mediates the overgrowth and anti-apoptotic effects by downregulating insulin-like growth factor-binding Protein-3 during nephroblastoma tumorigenesis. Fetal Pediatr Pathol. 35, 287–298.

Jiang, J., et al., 2018. Triptolide inhibits proliferation and migration of human neuroblastoma SH-SY5Y cells by up-regulating microRNA-181a. Oncol. Res. 26, 1235–1243.

Le Magnen, C., et al., 2013. Klf4 transcription factor is expressed in the cytoplasm of prostate cancer cells. Eur. J. Cancer 49, 955–963.

Lenarduzzi, M., et al., 2013. MicroRNA-193b enhances tumor progression via down regulation of neurofibromin 1. PLoS One 8, e53765.

Li, M.H., et al., 2008. Induction of antiproliferative connective tissue growth factor expression in Wilms' tumor cells by sphingosine-1-phosphate receptor 2. Mol. Cancer Res. 6, 1649–1656.

Li, J., et al., 2014. miR-193b directly targets STMN1 and uPA genes and suppresses tumor growth and metastasis in pancreatic cancer. Mol. Med. Rep. 10, 2613–2620.

Li, H., et al., 2015. Triptolide inhibits human breast cancer MCF-7 cell growth via downregulation of the ERalpha-mediated signaling pathway. Acta Pharmacol. Sin. 36, 606–613.

Li, P., et al., 2016a. MicroRNAs in laryngeal cancer: implications for diagnosis, prognosis and therapy. Am. J. Transl. Res. 8, 1935–1944.

Li, X., et al., 2016b. Triptolide reduces proliferation and enhances apoptosis of human non-small cell lung cancer cells through PTEN by targeting miR-21. Mol. Med. Rep. 13, 2763–2768.

Livak, K.J., Schmittgen, T.D., 2001. Analysis of relative gene expression data using real-time quantitative PCR and the 2(−Delta Delta C(T)) method. Methods. 25, 402–408.

Mets, E., et al., 2015. MicroRNA-193b-3p acts as a tumor suppressor by targeting the MYB oncogene in T-cell acute lymphoblastic leukemia. Leukemia. 29, 798–806.

Okuda, H., et al., 2013. miR-7 suppresses brain metastasis of breast cancer stem-like cells by modulating KLF4. Cancer Res. 73, 1434–1444.

Prabhu, R.H., et al., 2015. Polymeric nanoparticles for targeted treatment in oncology: current insights. Int. J. Nanomedicine 10, 1001–1018.

Reno, T.A., et al., 2015. Triptolide inhibits lung Cancer cell migration, invasion, and metastasis. Ann. Thorac. Surg. 100, 1817–1824 (discussion 1824-5).

Richards, M.K., et al., 2017. The association between nephroblastoma-specific outcomes and high versus low volume treatment centers. J. Pediatr. Surg. 52, 104–108.

Rowland, B.D., et al., 2005. The KLF4 tumour suppressor is a transcriptional repressor of p53 that acts as a context-dependent oncogene. Nat. Cell Biol. 7, 1074–1082.

Sarin, Y.K., Raj, P., 2015. Recurrent monophasic Wilms‘ tumor in pelvic kidney – a therapeutic challenge. APSP J. Case Rep. 6, 25.

Song, J.M., et al., 2017. Triptolide suppresses the in vitro and in vivo growth of lung cancer cells by targeting hyaluronan-CD44/RHAMM signaling. Oncotarget 8, 26927–26940.

Sun, Y., et al., 2016. NF-kappaB signaling plays irreplaceable roles in cisplatin-induced bladder cancer chemoresistance and tumor progression. Int. J. Oncol. 48, 225–234.

Sun, Y.Y., et al., 2017. Triptolide inhibits viability and induces apoptosis in liver cancer cells through activation of the tumor suppressor gene p53. Int. J. Oncol. 50, 847–852.

Tetreault, M.P., et al., 2010. Klf4 overexpression activates epithelial cytokines and inflammation-mediated esophageal squamous cell cancer in mice. Gastroenterology 139, 2124–2134.e9.

Tian, F., et al., 2014. The development of Wilms tumor: from WT1 and microRNA to animal models. Biochim. Biophys. Acta 1846, 180–187.

Wang, X.F., et al., 2014. Triptolide induces apoptosis in endometrial cancer via a p53independent mitochondrial pathway. Mol. Med. Rep. 9, 39–44.

Wang, J., et al., 2018. Triptolide inhibits pituitary adenoma cell viability, migration and invasion via ADAM12/EGFR signaling pathway. Life Sci. 194, 150–156.

Xiong, J., et al., 2016. Triptolide has anticancer and chemosensitization effects by down-regulating Akt activation through the MDM2/REST pathway in human breast cancer. Oncotarget. 7, 23933–23946.

Xu, C., et al., 2010. MicroRNA-193b regulates proliferation, migration and invasion in human hepatocellular carcinoma cells. Eur. J. Cancer 46, 2828–2836.

Yu, F., et al., 2011. Kruppel-like factor 4 (KLF4) is required for maintenance of breast cancer stem cells and for cell migration and invasion. Oncogene. 30, 2161–2172.

Zhang, J., et al., 2017. miR-193b-3p possesses anti-tumor activity in ovarian carcinoma cells by targeting p21-activated kinase 3. Biomed. Pharmacother. 96, 1275–1282.

Zhang, F.Z., et al., 2018. Triptolide, a HSP90 middle domain inhibitor, induces apoptosis in triple manner. Oncotarget. 9, 22301–22315.

Zhong, Q., et al., 2014. miR-193b promotes cell proliferation by targeting Smad3 in human glioma. J. Neurosci. Res. 92, 619–626.

Ziaei, S., Halaby, R., 2016. Immunosuppressive, anti-inflammatory and anti-cancer properties of triptolide: a mini review. Avicenna J. Phytomed. 6, 149–164.